Chapter 1

Effect of Microalloying Elements on the Heat Treatment Response and Tensile Properties of Al-Si-Mg Alloys

Mohamed F. Ibrahim, Mohamed H. Abdelaziz, Herbert W. Doty, Salvador Valtierra and Fawzy H. Samuel

Additional information is available at the end of the chapter

http://dx.doi.org/10.5772/intechopen.70665

Abstract

This study was carried out on a series of heat-treatable Al-Si-Mg alloys to determine the effects of Fe, Mg, Sr and Be addition on their microstructural characteristics and tensile properties. The results showed that the eutectic temperature was reduced by 10°C with 0.8 wt% Mg addition. The solidification curves and first derivatives of Sr-free alloys with high Fe and Mg contents revealed a peak at 611°C consequent to the formation of a script-like Be-Fe (Al8Fe2BeSi) phase, which was very close to the peak for α-Al. The morphology of the β-iron platelets underwent changes due to their dissolution, thinning, necking, and fragmentation with increase in solutionizing time. Increased Mg contents are beneficial to the tensile properties unlike the detrimental effect of increasing Fe contents. Additions of Be and Sr noticeably improved the properties at the same Fe and/or Mg contents, the enhancements being markedly observed at higher Mg contents and reduced Fe levels. At high Fe levels, addition of Be is preferable as it neutralizes the deleterious effects of Fe in these alloys; however, addition of 500 ppm Be is inadequate for interacting with other alloying elements.

Keywords: aluminum alloys, Minitab, scattered plot, intermetallics, Si coarsening

1. Introduction

The main objectives of heat-treating cast Al-Si-Mg alloys include homogenization, stress relief, improved dimensional stability, and optimization of the strength and ductility parameters. The T6 heat-treated Al-Si-Mg alloys have an optimum combination of strength and ductility.

The typical heat treatment specification of a T6 temper consists of solid solution treatment and quenching, followed by aging. The main effects of solution heat treatment are the dissolution of Mg_2Si particles, the homogenization of the casting, and modification of the morphology of eutectic silicon through fragmentation and spheroidization at critical temperatures. The recommended solution temperature for 356 and 357 alloys is 540 ± 5°C [1, 2].

The purpose of quenching is to preserve the solid solution formed at the solution heat treatment temperature by rapid cooling to room temperature. The quenching medium and rate are the parameters which control the mechanical properties. The highest strength can be ensured when the material is subjected to a rapid quenching rate. Aging is the final stage of heat treatment in cast Al-Si-Mg alloys. The aging can be natural or artificial. Alloy mechanical properties depend on both aging temperature and time. The main objective of artificial aging is to heat the as-quenched castings to an intermediate temperature between 150 and 200°C for 4–8 h in order to precipitate the excess solutes which were supersaturated in α-Al during the solution heat treatment process. The improvement achieved in the mechanical properties during artificial aging is due to the precipitation of metastable phases from the supersaturated solution. Al-Si-Mg alloys fulfill the following precipitation sequence [3]:

SS → needle-shaped GP zones → rod-like β' precipitates → platelets of Mg_2Si.

For Al-Si-Mg alloys, the solubility of Mg and Si in the Al matrix decreases with temperature. In order to obtain a maximum concentration of Mg and Si particles in solid solution, the solution temperature should be close to the eutectic temperature. For the 356 and 357 alloys, the solution temperature is 540 ± 5°C. At this temperature, about 0.6% Mg can be placed in solid solution. The dissolution of Mg_2Si into Mg and Si occurs in the two alloys at 475 and 540°C, respectively [4].

An investigation [5] was carried out on the effects of T6 and T4 tempers on the tensile properties of nonmodified and Sr-modified A356 alloys obtained from permanent mold and sand mold castings. The results showed that the yield strength is not appreciably influenced by the change in Si-particle characteristics. The ultimate tensile strength (UTS) and %El increases significantly with increase in the solution treatment time at 540°C. Also it was observed that upon modification with Sr the fracture mode changes from brittle to ductile especially in sand castings. Both non-modified and Sr-modified alloys obtained from permanent mold casting, however, showed ductile fracture mode. All the improvements in the tensile properties reported upon were related mainly to the changes which occurred in the Si particle aspect ratio and particle size during solution treatment.

Yoshida and Arrowood [6] studied the effects of varying the solutionizing parameters (time and temperature) of a T6 traditional treatment on the mechanical properties (i.e., hardness, ductility, and ultimate tensile strength) of Sr-modified and nonmodified permanent mold cast A356 alloys. The investigated solution treatment times were 2, 4, 8, 16, and 32 h, while the solution treatment temperatures were 520 and 540°C, where the aging treatment was kept unchanged at 160°C for 6.5 h. The highest hardness was obtained at the shortest solutionizing time of 2 h for both the unmodified and modified A356 alloy, while the highest ductility was

not reached until the samples were solutionized for 8 h at the same temperature. A slight change in solutionizing temperature did not cause much variation in hardness, ductility, or UTS. It may also be concluded that the Sr-modified samples exhibit higher ductility than the unmodified ones under all the heat treatment conditions reported in this study.

A valuable study was carried out by Moustafa et al. [7, 8] on A413. 1 Al-Si eutectic alloys, where they reported that alloys with Mg contents suffered reduction in hardness, yield strength, and ultimate tensile strength values following the addition of Sr. They explained this observation in terms of retarded precipitation of Mg_2Si particles during the aging treatment owing to longer incubation period preceding the commencement of precipitation, irrespective to the solutionizing time [8, 9]. Also, alloying element additions of Mg and Be, resulted in improving the hardness and strength of the base alloy, especially in the T6 condition, where adding small amount of Be (~0.02%) prevented Mg oxidation (i.e., formation of MgO and $MgAl_2O_4$ (spinel)) during melting, so that the hardness increased slightly.

The main purpose of this study, on Al-Si-Mg type 356 and 357 casting alloys, is to investigate the effects of alloying elements and heat treatment conditions on the microstructure and mechanical behavior of nonmodified and Sr-modified 356- and 357-type alloys by examining the following factors:

1. The influence of alloying elements on the aging behavior of alloy castings investigated in relation to:
   a. Fe content, Sr-modification, grain refining, and addition of Mg and Be; and
   b. Solution heat treatment and aging parameters.
2. Microstructural analysis of the precipitated phases during the solidification process.
3. Correlating the results obtained from the tensile testing with the microstructural analysis to determine the effects of each alloying element, intermetallic phase, changes in the morphology, solutionizing parameter, and aging condition on the mechanical properties of the alloys investigated.

2. Experimental procedure

The chemical composition of the B356.2 alloy used in the present study is shown in **Table 1**. The Mg level of the alloy was increased by adding pure Mg to the alloy melts to obtain Mg levels of 0.4, 0.6, and 0.8 wt%. The Fe and Be were added in the form of Al-25% Fe and Al-5% Be master alloys, respectively, to the alloy melt to obtain Fe levels of 0.09, 0.2, and 0.6 wt% and a Be level of 0.05 wt%. The Sr and Ti were added in the form of Al-10% Sr and Al-5% Ti master alloys, for Sr-modification and grain refining purposes, respectively, to the alloy melts to obtain levels of 0.02 wt% Sr and 0.15 wt% Ti.

AA alloy no.*	Chemical composition (wt%)**					
	Si	Fe	Cu	Mg	Zn	Al
B356.2	7.0	<0.06	<0.025	0.35	<0.001	Bal

*AA, aluminum association.

**Unlisted aluminum or impurities.

Table 1. Chemical composition of the B356.2 alloy (wt%) [8].

An electrical resistance furnace with a 70-kg crucible capacity was used to prepare 60 kg of each alloy. The melt was kept at 750 ± 5°C as the melting temperature at which additions of magnesium, iron, beryllium, strontium, and titanium were made. These measured additions were added to the melt using a perforated graphite bell. Before casting, the melt was degassed using pure and dry argon for 20 min using a graphite impeller in order to clean the melt from hydrogen and inclusions. For the purposes of thermal analysis, one sample of each alloy composition was prepared using the arrangement shown in **Figure 1**; moreover, two samplings for chemical analysis were also taken from each melt, one before the start of casting and one at the end of casting.

The chemical analysis was carried out using arc spark spectroscopy at GM facilities in Milford, NH. The actual chemical composition of each of the alloys prepared is shown in **Table 2**, representing average values taken over three spark measurements made for each chemical analysis sample. The alloys A1 through C3B shown in the table represent 18 non-modified alloys

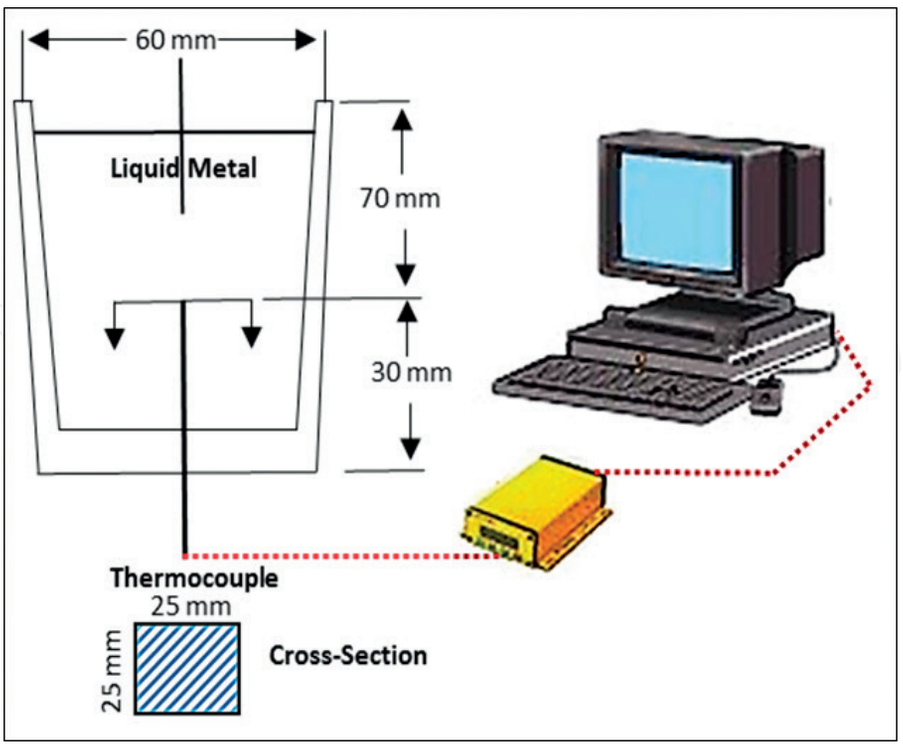

Figure 1. Schematic drawing showing the graphite mold used for thermal analysis.

http://dx.doi.org/10.5772/intechopen.70665

Alloy code	Element concentration (wt%)								
	Si	Fe	Mg	Cu	Mn	Ti	Sr	Be	Al
A1*	7.02	0.101	0.376	0.050	0.010	0.143	0.001	—	Bal.
B1	7.00	0.203	0.383	0.008	<0.001	0.151	0.001	—	Bal.
C1	6.97	0.630	0.372	0.011	0.002	0.174	0.001	—	Bal.
A2	6.99	0.113	0.590	0.042	0.008	0.164	0.001	—	Bal.
B2	7.03	0.210	0.570	0.009	0.002	0.179	0.001	—	Bal.
C2	6.88	0620	0.540	0.010	0.002	0.172	0.001	—	Bal.
A3	7.08	0.123	0.760	0.034	0.007	0.192	0.002	—	Bal.
B3	7.35	0.226	0.750	0.009	0.002	0.197	0.001	—	Bal.
C3	7.07	0.630	0.750	0.010	0.003	0.183	0.002	—	Bal.
A1B*	7.33	0.093	0.368	0.052	0.006	0.180	0.001	0.034	Bal.
B1B	6.61	0.197	0.474	0.011	<0.001	0.180	0.001	>0.036	Bal.
C1B	6.89	0.670	0.510	0.011	0.002	0.186	0.003	>0.036	Bal.
A2B	7.26	0.081	0.530	0.006	<0.001	0.173	0.001	>0.036	Bal.
B2B	6.60	0.184	0.710	0.007	<0.001	0.177	0.001	>0.036	Bal.
C2B	6.22	0.680	0.700	0.007	0.002	0.183	0.001	>0.036	Bal.
A3B	6.50	0.127	0.980	0.034	0.006	0.203	0.001	0.026	Bal.
B3B	6.38	0.196	0.960	0.009	0.001	0.210	0.001	>0.036	Bal.
C3B	5.96	0.560	0.920	0.009	0.003	0.221	0.002	>0.036	Bal.
A1S	7.06	0.103	0.338	0.046	0.010	0.139	0.016	—	Bal.
B1S	7.18	0.217	0.354	0.014	0.002	0.165	0.019	—	Bal.
C1S	7.18	0.660	0.349	0.007	0.002	0.172	0.017	—	Bal.
A2S	7.07	0.105	0.520	0.033	0.002	0.156	0.018	—	Bal.
B2S	7.26	0.217	0.530	0.009	0.001	0.169	0.015	—	Bal.
C2S	7.17	0.640	0.530	0.008	0.002	0.154	0.017	—	Bal.
A3S	7.98	0.101	0.820	0.035	0.002	0.152	0.013	—	Bal.
B3S	7.26	0.185	0.730	0.030	0.002	0.171	0.009	—	Bal.
C3S	6.84	0.710	0.860	0.034	0.005	0.169	0.006	—	Bal.
A1BS	6.54	0.122	0.640	0.041	0.007	0.227	0.048	>0.036	Bal.
B1BS	6.12	0.190	0.491	0.009	<0.001	0.217	0.027	>0.036	Bal.
C1BS	7.78	0.810	0.530	0.084	0.012	0.210	0.016	>0.036	Bal.
A2BS	7.64	0.123	0.780	0.010	0.002	0.243	0.024	>0.036	Bal.
B2BS	5.93	0.194	0.730	0.007	<0.001	0.227	0.023	>0.036	Bal.
C2BS	7.06	0.670	0.710	0.007	0.002	0.222	0.022	>0.036	Bal.

Alloy code	Element concentration (wt%)								
	Si	Fe	Mg	Cu	Mn	Ti	Sr	Be	Al
A3BS	7.26	0.105	0.950	0.020	0.002	0.188	0.023	>0.036	Bal.
B3BS	6.33	0.194	0.950	0.021	0.002	0.189	0.017	>0.036	Bal.
C3BS	6.21	0.690	0.850	0.033	0.005	0.207	0.014	>0.036	Bal.

Table 2. Average chemical composition (wt%) of the alloys studied.

while their Sr-modified counterparts were coded A1S to C3BS, respectively. The Sr level ranged from 0 to 0.02 wt% in these alloys. The codes A, B, C, 1, 2, etc. are explained below.

A = 0.1% Fe, B = 0.2% Fe, C = 0.6% Fe, 1 = 0.4%Mg, 2 = 0.6% Mg, 3 = 0.75% Mg, S = Sr,*B = Be.

The various alloys were used to prepare castings from which test bars were obtained for tensile testing purposes. With this aim in mind, the degassed molten metal was carefully poured into an ASTM B-108 permanent mold preheated to 450°C, to obtain castings for tensile testing. **Figure 2a** shows the actual casting obtained whereas **Figure 2b** shows the dimensions of the tensile bars.

Following casting in the ASTM B-108 permanent mold, the tensile bars were divided into 13 different bundles (5 bars/bundle); each bundle was subjected to certain heat treatment conditions as follows: 1 bundle was kept in the as-cast condition; 1 bundle was solution treated at 540°C for 5 h, then quenched in warm water at 65°C, and was kept in the as-solutionized condition; another bundle was kept also in the as-solutionized condition, however, after solutionizing for 12 h at 540°C followed by quenching in warm water at 65°C; 5 bundles were solution heat-treated at 540°C for 5 h, then quenched in warm water at 65°C followed by artificial aging at 160°C for 2, 4, 6, 8, and 12 h, respectively; the remaining 5 sets (bundles) were solution heat-treated at 540°C for 12 h, then quenched in warm water at 65°C followed by artificial aging at 160°C for 2, 4, 6, 8, and 12 h, respectively. The solution and aging heat-treatments were carried out in a forced-air Blue M electric furnace equipped with a programmable temperature controller, accurate to ±2°C. The aging delay was less than 10 s. For each individual heat treatment, five test bars were used.

For each condition, the test bars were pulled to fracture at room temperature at a strain rate of 4×10^{-4}/s using an MTS Servohydraulic mechanical testing machine. During the course of the tensile test, an attachable strain-gauge extensometer was connected to the gauge section of the tensile bars to measure the percentage elongation. The reported tensile data were the percentage elongation to fracture (%EF), 0.2% offset yield strength, and ultimate tensile strength; these data were reported as the average values of five data sets obtained from pulling five bars per condition.

Samples for microstructural analysis were taken from both the tensile-tested bars ~10 mm below the fracture surface and the as-cast thermal analysis castings, which were sectioned to study each alloy condition, that is, for the tensile-tested bars, one sample was used in the as-cast condition, while the other two were solution heat-treated (540°C/5 h and 540°C/12 h) beside the as-cast thermal analysis sample. The microstructures of the polished sample

http://dx.doi.org/10.5772/intechopen.70665

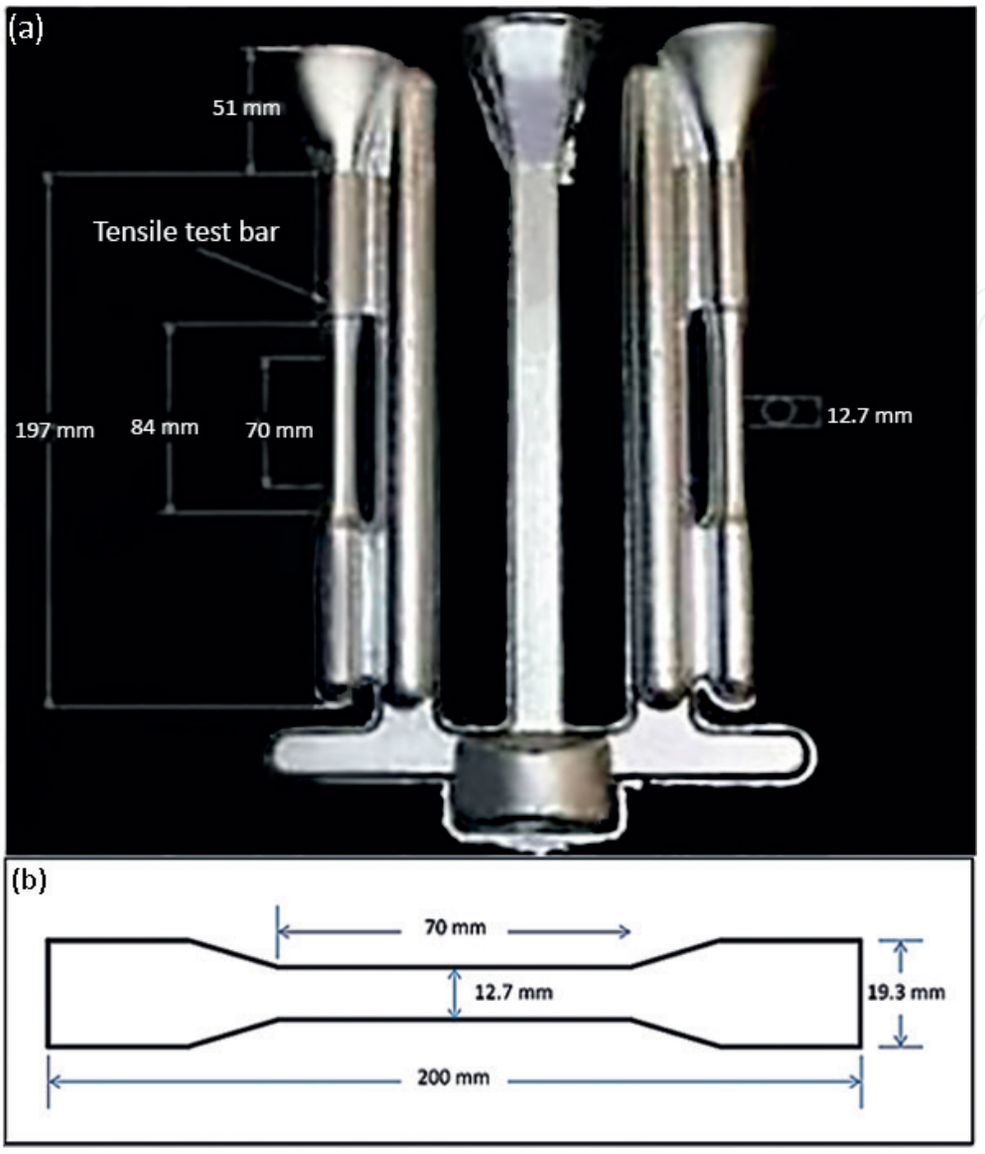

Figure 2. (a) ASTM B-108 permanent mold used for casting tensile test bars and (b) dimensions of the tensile test bar (in mm).

surfaces were examined using an optical microscope linked to a Clemex image analysis system, and a Hitachi S-4700 field emission scanning electron microscope (FE-SEM), equipped with a standard secondary electron detector (SE), a backscatter electron detector (BSD), and an energy dispersive X-ray spectrometer (EDS).

3. Results and discussion

3.1. Eutectic Si particles

Measurements of the dendrite arm spacing (DAS) showed that the DAS was about 24 μm in the as-cast tensile bars. The Si particle measurements for the A1 base alloy, containing

low levels of Mg and low Fe, and modified base alloy A1S, show that the Si particle area decreased from 28.4 to 0.67 μm², the Si particle length decreased from 10.8 to 1.25 μm (as can be seen from **Figure 3**), the aspect ratio decreased from 3.78 to 1.84, while the roundness ratio increased from 18.9 to 50.3% upon addition of Sr to the A1 base alloy in the as-cast condition [9–14].

The addition of Be in alloy A1B1 resulted in reduced silicon particle area of 10.3 μm², a reduced silicon particle length of 6.6 μm, a lower value of aspect ratio (2.73), and an increased roundness ratio up to a value of 35.7%. The mutual addition of Sr and Be (alloy A1BS) led to a reduction in silicon particle area (1.31 μm²), silicon particle length (1.84 μm), and the aspect ratio (1.94); however the roundness ration increased to 47.6%. By increasing the Fe and Mg content (alloy C3), the silicon particle area decreased to 6.9 μm², the silicon particle length and aspect ratio reduced to 6.44 μm and 3.01, respectively, while the roundness ratio increased to 24.6%. The combined addition of strontium, beryllium, iron, and magnesium (alloy C3BS) reduced the silicon particle area to 1.53 μm², the silicon particle length to 2 μm, the aspect ratio to 1.99 and increased the value of the roundness ratio to 46.7%. The aforementioned values of the silicon particle characteristics highlight the modification effect of Sr and the partial modification effect of both Mg and Be. However, with increasing Fe levels it seems that most of the Be reacts with the Fe forming a Be-Fe phase (Al8Fe2BeSi). The results for the average Si particle length are summarized in **Figure 3**.

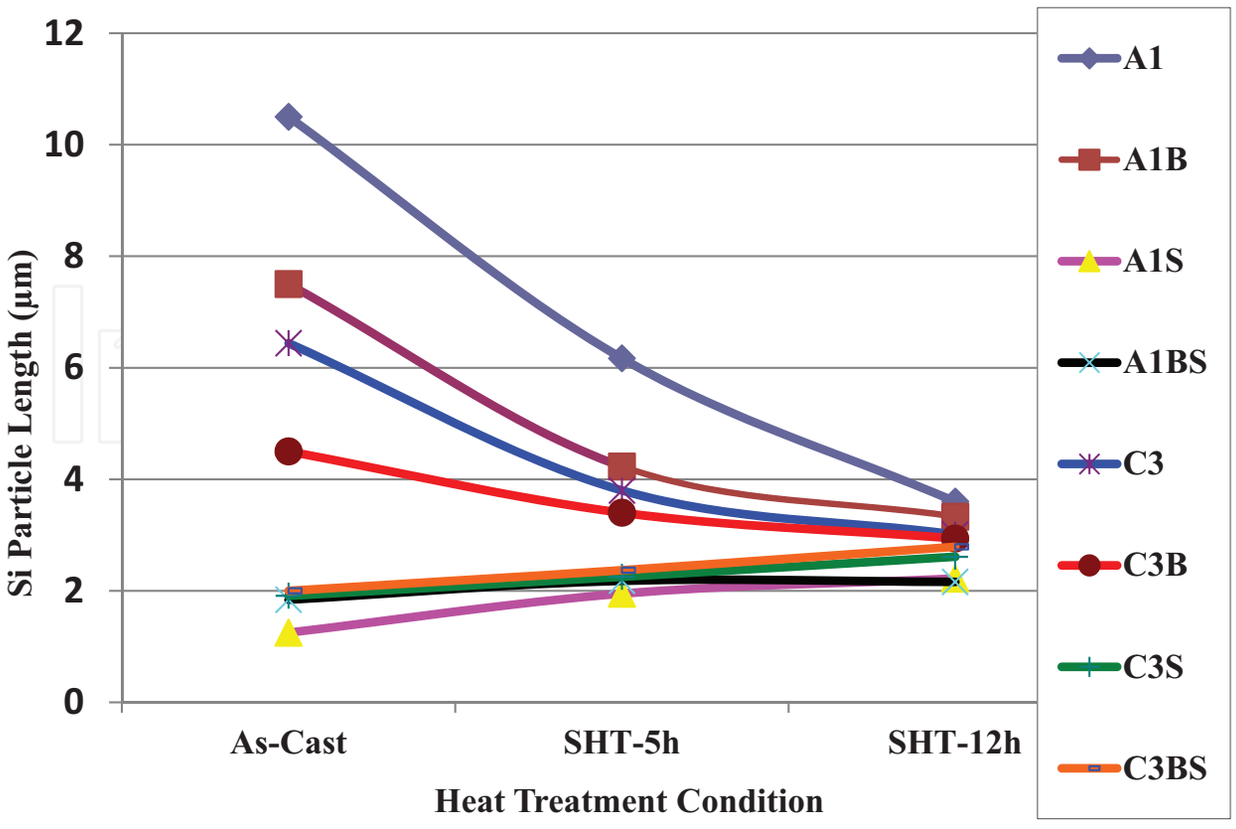

Figure 3. Average length of eutectic silicon particles with different solution heat treatment conditions.

Figure 4 shows the morphology of the eutectic Si particles in the A1 alloy, deeply etched in hydrofluoric acid (HF) solution. As can be seen in **Figure 4a**, the Si particles precipitated in the form of short platelets with sharp angles (white arrow). Solutionizing at 540°C resulted in fragmentation of the Si particles as demonstrated by the circled area in **Figure 4b**. As inferred from **Figure 4c**, there is a large difference in the particle sizes (see arrow) caused by dissolution of these particles in the aluminum matrix leading to coarsening of the other particles and hence the reported standard deviation (100%). Another observation that could be made from **Figure 4c** is that the new fragments of the Si platelets are still maintaining the platelet shape as shown by the more elongated particles in the figure. This process continued even after solutionizing for 400 h at 540°C as displayed in **Figure 4d–f**.

Figure 5 shows the microstructure of A1S alloy. As expected, addition of Sr 160 ppm resulted in changing the morphology of the Si particles to fibrous as displayed in **Figure 5a**. The microstructure of the A1S alloy following solutionizing at 540°C for 5 h is presented in **Figure 5b**. Three observations could be made from this figure:

i. Necking of the Si particles-solid arrow

ii. Dissolution of some particles in the matrix-broken arrow, in keeping with the: Ostwald ripening mechanism [15] (see **Figure 6**).

iii. Coarsening of other particles by collision.

Increasing the solutionizing time to 12 h at 540°C led to partial spheroidization as shown by the solid arrows in **Figure 5c** where the new particles are having multiple sides. The white area circled in **Figure 5c** points to particle collision. **Figure 5d** is an enlarged portion of **Figure 5c** showing the possibility of the fusion of some particles in the background to the left, leading to a coarser one. This process of coarsening was observed to continue up to 400 h at 540°C, **Figure 5d–f**. It should be noted here that the Si particles are not spherical; rather, they possess multiple faces (**Figure 5f**).

3.2. Precipitation of Mg_2Si

Samuel et al. [16] observed that any Sr-modified microstructure is clearly affected when magnesium is present. Microstructural parameters as obtained from image analysis, such as silicon particle size and aspect ratio, were found to increase with an increasing Mg content, subsequently becoming increasingly inhomogeneous. The reason for the deterioration in modification is believed to be the formation of intermetallic phases of the type $Mg_2SrAl_4Si_3$, where the addition of Mg also lowers the eutectic temperature - the eutectic temperature decreases with increasing Mg content. It was also reported, however, that a magnesium content of ~1 wt% itself acts as a refiner for the eutectic silicon in unmodified Al-Si alloys.

Ibrahim et al. [17] showed that the addition of up to 0.5 wt% of Mg to molten 319 type alloys results in the formation of Mg_2Si; the Mg-rich phase commonly exists as rounded black particles close to the eutectic silicon particles. It was also reported that the addition of Mg results in remarkable fragmentation/modification of the eutectic silicon particles as well as transformation of a large portion of the harmful needles of β-Al_5FeSi Fe phase into the less detrimental Chinese script-like phase with a composition close to $Al_8Mg_3FeSi_6$.

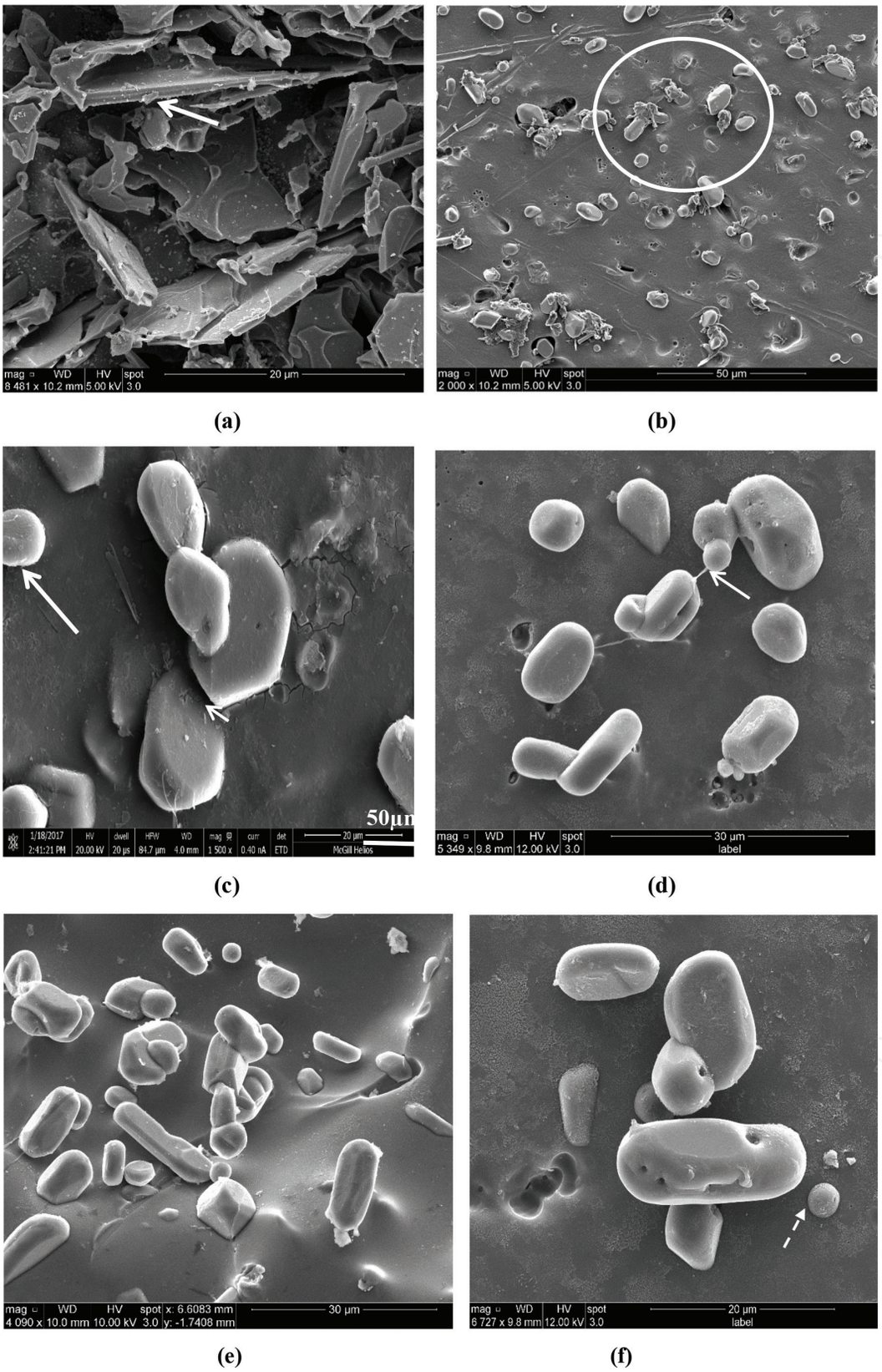

Figure 4. Variation in eutectic Si particles in A1 alloy as a function of heat treatment: (a) as cast, (b and c) after 5 h at 540°C, (d) after 12 h at 540°C, (e) after 200 h at 540°C, and (f) after 400 h at 540°C. The white arrow in (f) reveals the dissolution of fine particles even after the long solutionizing time at 540°C.

http://dx.doi.org/10.5772/intechopen.70665

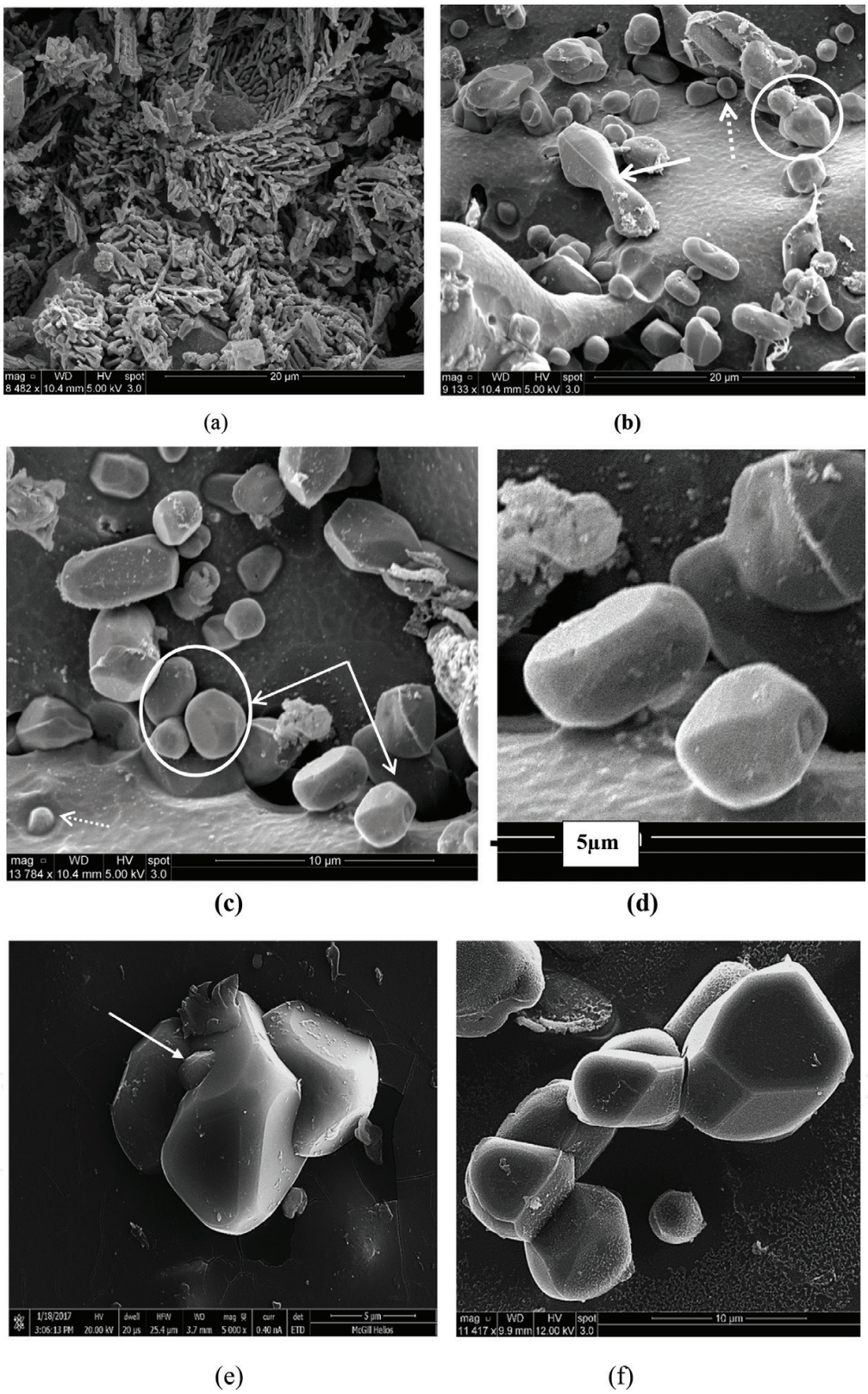

Figure 5. Variation in eutectic Si particles in A1S alloy as a function of heat treatment: (a) as cast, (b) after 5 h at 540°C, (c and d) after 12 h at 540°C, and (e) after 200 h at 540°C, and (f) after 400 h at 540°C broken arrow in (b) points to the presence of very small Si particles, whereas the solid arrow in (e) indicates the complete fusion of a Si particle in a cluster of particles.

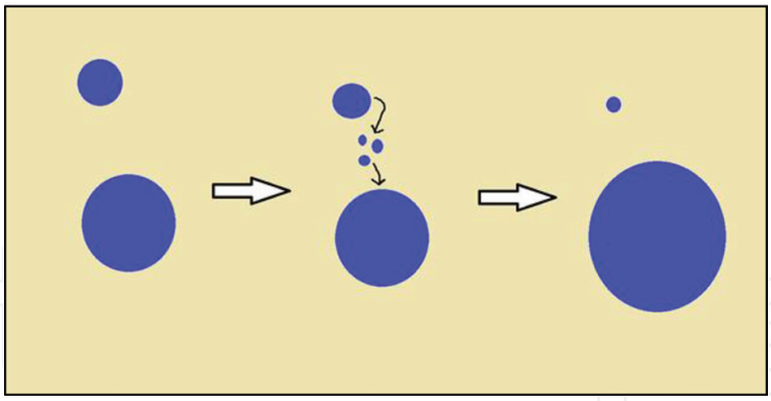

Figure 6. Schematic diagram showing coarsening of Si particles according to Ostwald ripening mechanism [15].

The heat treatment for Al-Si-Mg alloy is T6 which consists of solution heat treatment and natural or artificial aging. A solution treatment between 400 and 560°C, results in the dissolution of the hardening phase (Mg_2Si) in the aluminum matrix. However, the solutionizing temperature is limited by the eutectic phase melting temperature. The alloy thereafter is aged at low temperature (150–200°C) for precipitation of the hardening compounds which improves the mechanical properties of the aluminum matrix [18]. The primary purpose of the long solution treatment is to thermally alter silicon particle characteristics [19]. During T6 treatment, the Mg and Si which are in solid solution precipitate as Mg_2Si during the aging treatment [13].

Figure 7a reveals the precipitation of Mg_2Si in the form of Chinese script (black) following the formation of π-$Al_8Mg_3FeSi_6$ in 356 alloy solidified at 0.8°C/s (A1 alloy). The identity of these two phases was confirmed from their corresponding EDS spectra shown in **Figure 7b** and **c**, respectively. The microstructure of the A1 alloy following solutionizing at 540°C for 12 h is shown in **Figure 8a**, revealing the presence of scattered particles. These particles have been identified as Si particles [20]. Following aging at 160°C for 12 h resulted in the dense precipitation of Mg_2Si particles in the form of short rods-**Figure 8b**. Obviously, the density of the Mg_2Si precipitation is controlled by the amount of added Mg and the presence of Sr [21]. Another parameter to be considered during long solutionizing times is the decomposition of the π-phase into the β-phase as demonstrated in **Figure 9** [22].

3.2.1. Tensile properties

Tensile properties of reference alloys A1, A3, and C3 in the as-cast and different heat treatment conditions applied are summarized in **Table 3**. In the as-cast samples, increasing Mg content from 0.4 wt% (base alloy A1) to 0.8 wt% (alloy A3) resulted in slightly increasing the strength due to the partial modification effect of Mg as well as the transformation of β-phase to π-phase, that is, most of the Fe-intermetallic phases precipitated in the form of the π-phase in spite of the low Fe content (0.09 wt%), whereas increasing the Fe level up to 0.6 wt% in the high Mg-containing alloy A3 i.e. alloy C3 resulted in decreasing the UTS somewhat, because of the growing formation of Fe-intermetallic phases. For the three reference alloys, percent elongation was decreased.

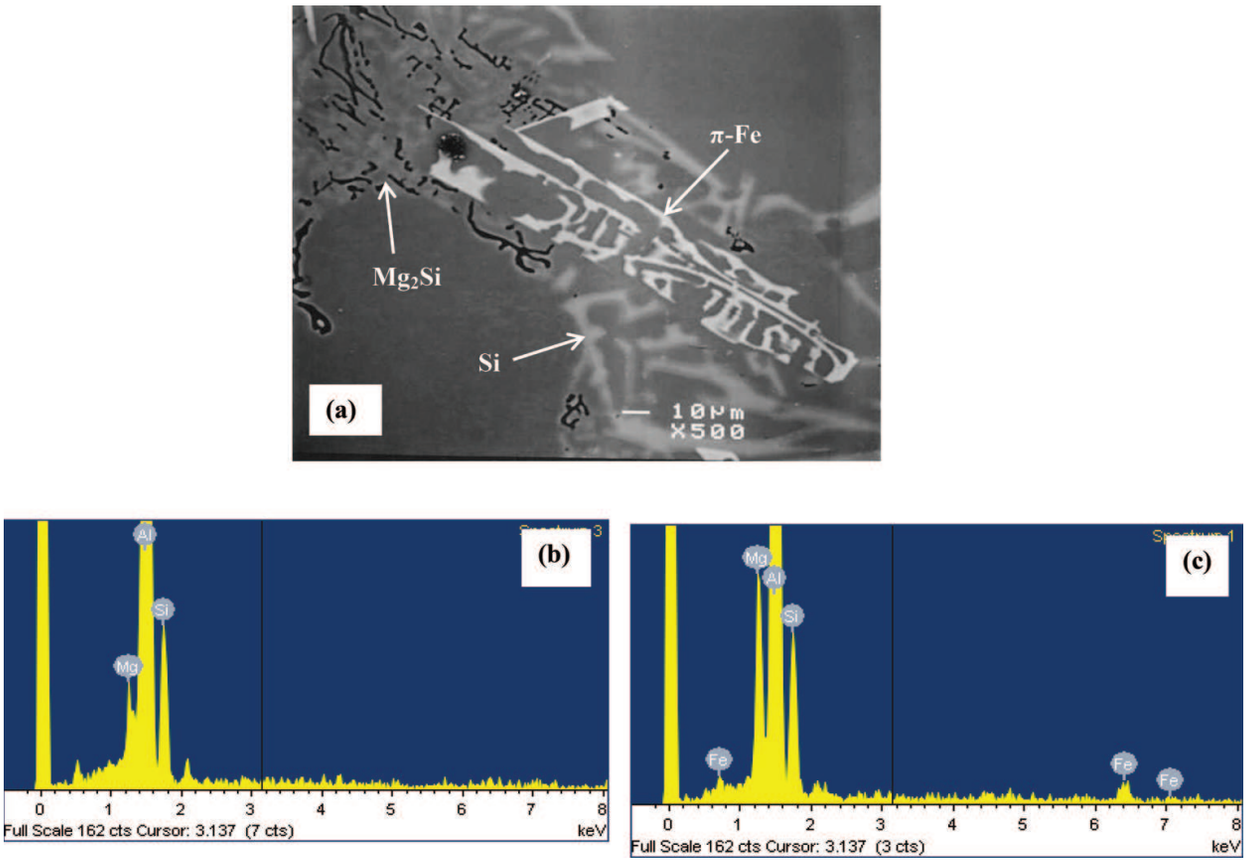

Figure 7. Precipitation of Mg_2Si and π-Fe in 356 alloy solidified at 0.8°C/s: (a) backscattered electron image, (b) EDS spectrum corresponding to Mg_2Si phase, and (c) EDS spectrum corresponding to π-phase.

Applying 5 h solution heat treatment at 540°C appeared in a noticeable increase in the ultimate strength (UTS) values, (59 MPa) for alloys A1 and A3, and (39 MPa) for alloy C3, due to the fragmentation and spheroidization of Si particles and spheroidization of undissolved π-phases as well as dissolving of Mg_2Si in the matrix and the decomposition of the π-phase to β-phase which further fragmented during solution heat treatment, thereby improving the tensile properties. For both solutionizing times, the elongation values obtained were two times or more higher than those observed in the as-cast condition for alloys A1, A3, and C3, indicating improved ductility of the solution heat-treated samples. Similar results regarding the addition of alloying elements and solution heat treatment parameters have been reported in a number of studies [23–30].

The tensile data of the 31 alloys used in the present work was classified into 4 series:

1. Fe-Mg series.
2. Fe-Mg-Be series.
3. Fe-Mg-Be-Sr series.
4. Fe-Mg-Sr series.

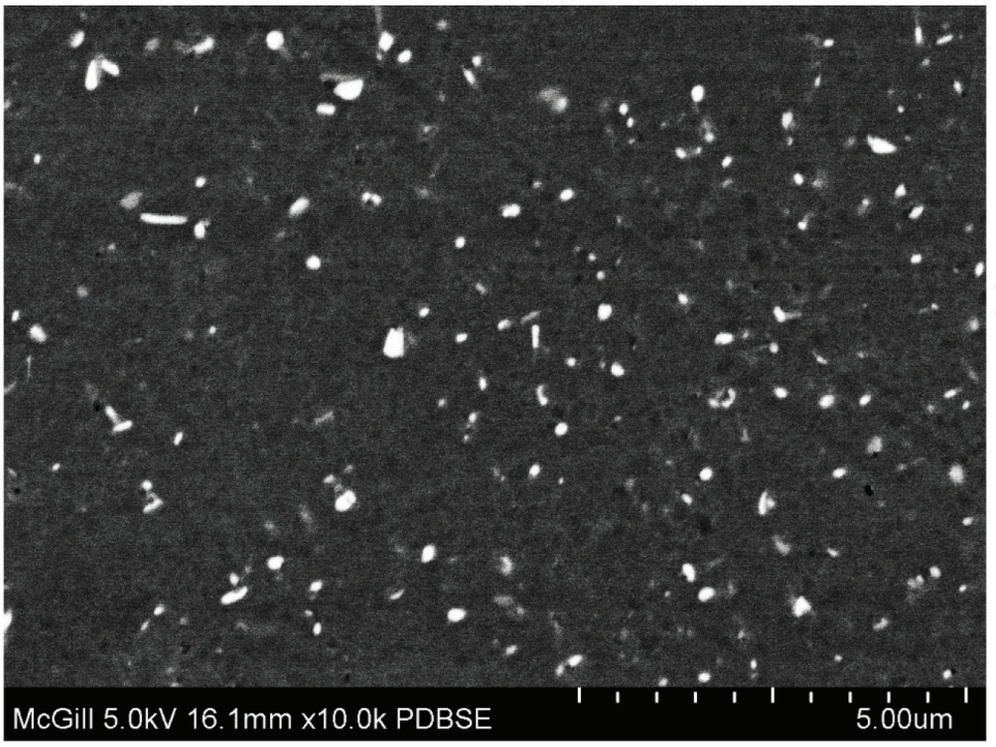

(a)

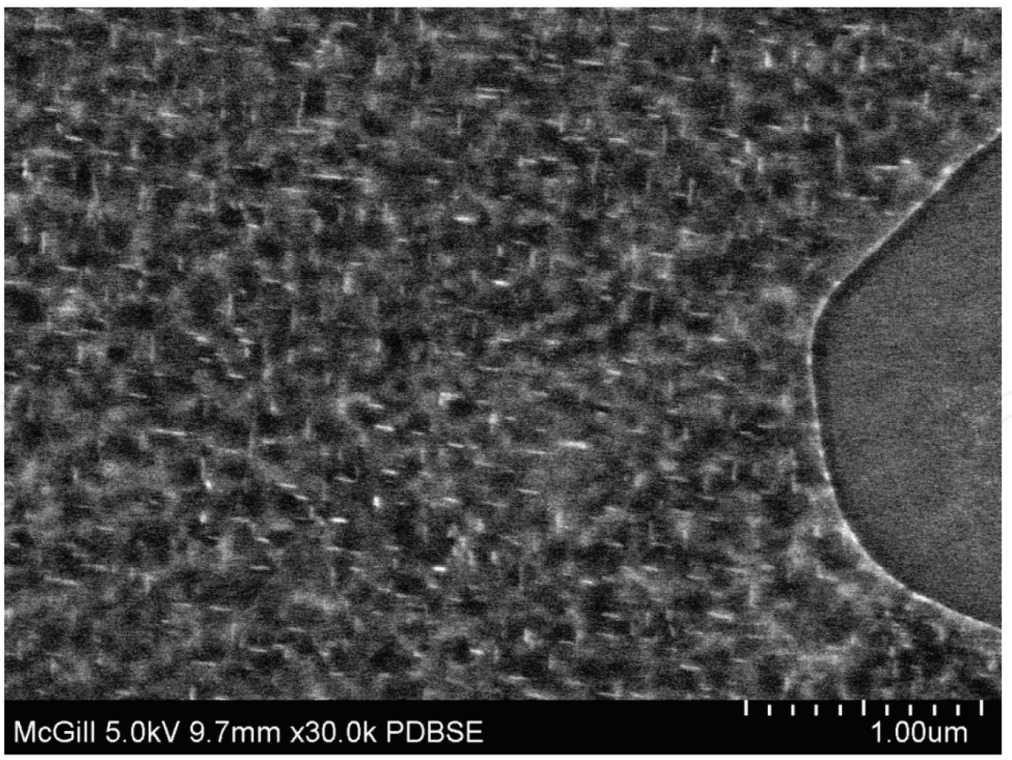

(b)

Figure 8. Backscattered electron images of the precipitation observed in A1 alloy tensile bars: (a) T4 condition and (b) T6 condition.

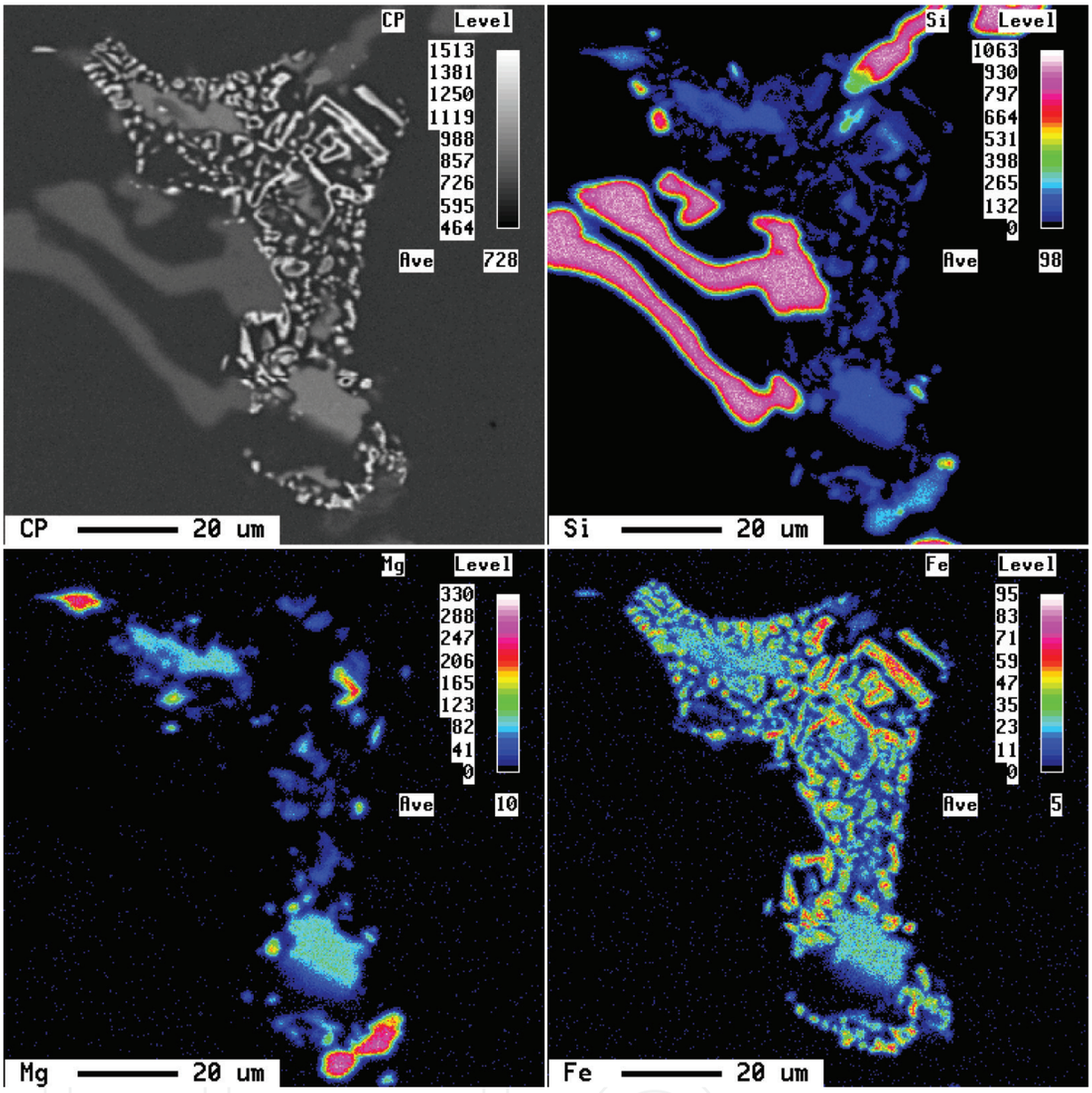

Figure 9. Decomposition of π-phase to β-phase during solutionizing at 540°C for 12 h [22].

The data was then treated using Minitab software and is presented in **Figures 10–12**.

Based upon the results presented in these figures, the following observations may be noted:

1. In the as-cast condition, increasing the Mg content leads to further transformation of the β-phase platelets to a Chinese script π-phase, regardless of the Fe content, thereby decreasing the harmful effect of the β-phase.
2. Increasing the solution heat treatment time leads to further decomposition of the π-phase, fragmentation of the β-phase, and spheroidization of the eutectic Si, resulting in an improvement in the alloy tensile properties.

3. Increasing the Fe level decreases the alloy ductility values, whereas the addition of Mg increases the % EF-values.

4. Introducing Be, Sr, or both, improves the alloy strength to some extent, regardless of the levels of Fe and Mg present.

5. Increasing solution treatment time from 5 to 12 h enhances the UTS and YS values.

6. Increasing the Mg-content results in improving the tensile properties; however increasing the iron levels markedly deteriorates these properties.

7. Additions of Be and Sr noticeably improves the mechanical properties of the alloys with the same Fe and/or Mg contents; however, these enhancements in mechanical properties are markedly observed at higher Mg contents and reduced levels of Fe.

Alloy code	**Property**	**As-cast**	**SHT 5 h**	**Aging time (h)—SHT 5 h**				
				2	**4**	**6**	**8**	**12**
A1	UTS (MPa)	204	262	342	358	361	354	360
	YS (MPa)	97	116	237	267	277	282	292
	El (%)	6.5	15.9	10	8.7	8.1	6.2	6.5
A3	UTS (MPa)	204	263	343	358	381	383	386
	YS (MPa)	114	141	254	292	330	333	347
	El (%)	3.4	7.2	5.96	4.3	3.1	2.8	2.0
C3	UTS (MPa)	201	239	320	328	366	366	360
	YS (MPa)	116	135	270	297	345	350	357
	El (%)	2.6	4.8	1.7	1.0	1.0	0.9	0.7
Alloy code	**Property**	**As-cast**	**SHT 12 h**	**Aging time (h)—SHT 12 h**				
				2	**4**	**6**	**8**	**12**
A1	UTS (MPa)	204	255	340	358	360	362	362
	YS (MPa)	97	107	229	273	284	274	280
	El (%)	6.5	17.6	12.3	10	8.7	9.5	8.5
A3	UTS (MPa)	204	287	351	368	382	382	384
	YS (MPa)	114	154	266	295	321	336	353
	El (%)	3.4	9.7	6.5	3.6	4.0	2.7	2.0
C3	UTS (MPa)	201	250	317	334	367	365	364
	YS (MPa)	116	152	294	301	317	326	327
	El (%)	2.6	4.3	1.0	1.0	0.9	0.7	0.7

Table 3. Tensile properties of reference alloys A1, A3, and C3 in the as-cast and heat-treated conditions.

http://dx.doi.org/10.5772/intechopen.70665

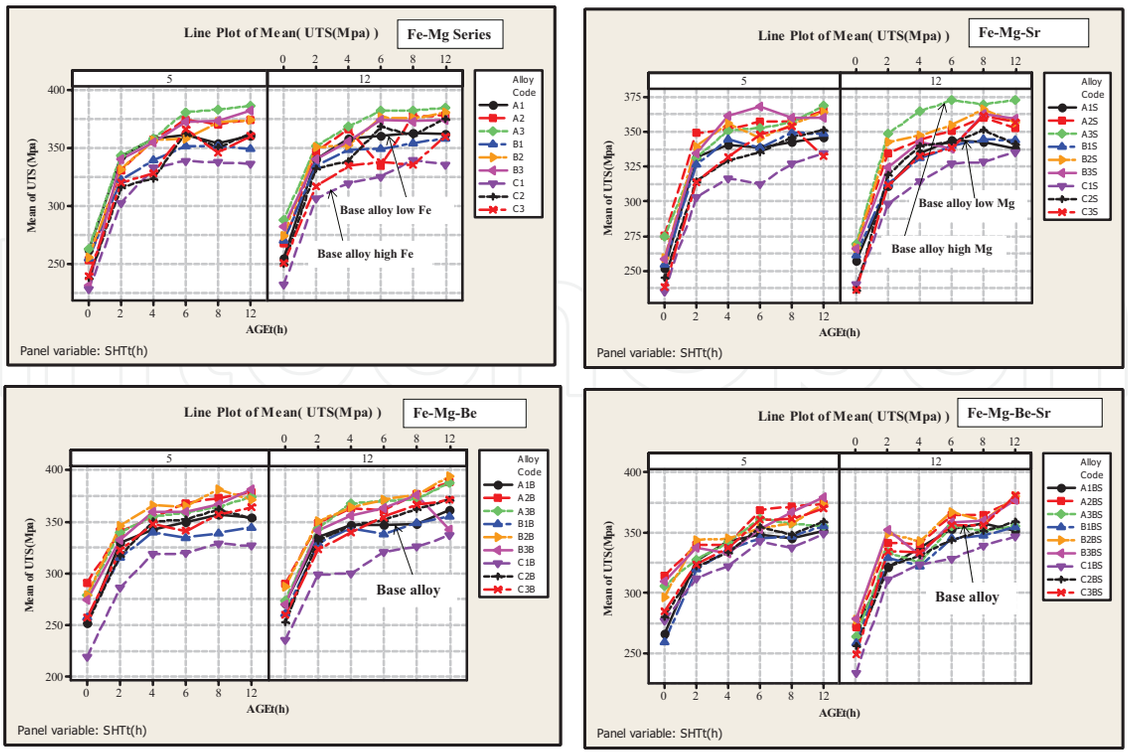

Figure 10. Variation in the UTS values as a function of alloying elements.

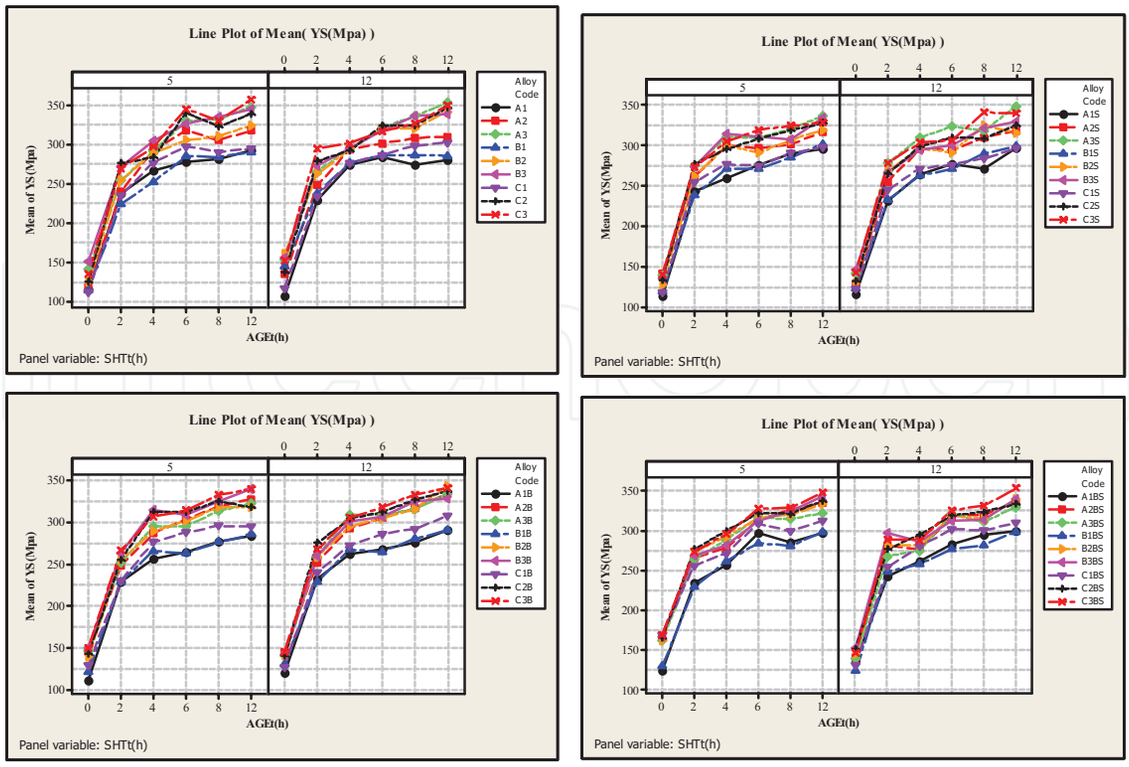

Figure 11. Variation in the YS values as a function of alloying elements.

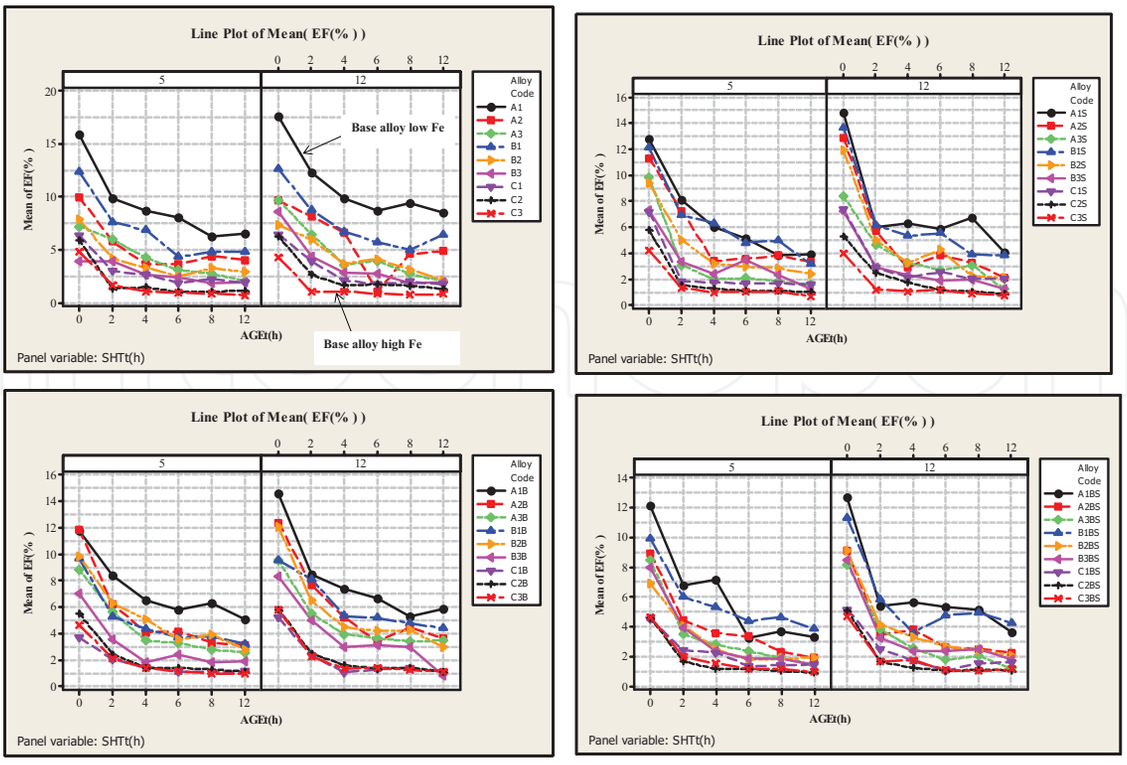

Figure 12. Variation in the % elongation to fracture (EF) values as a function of alloying elements.

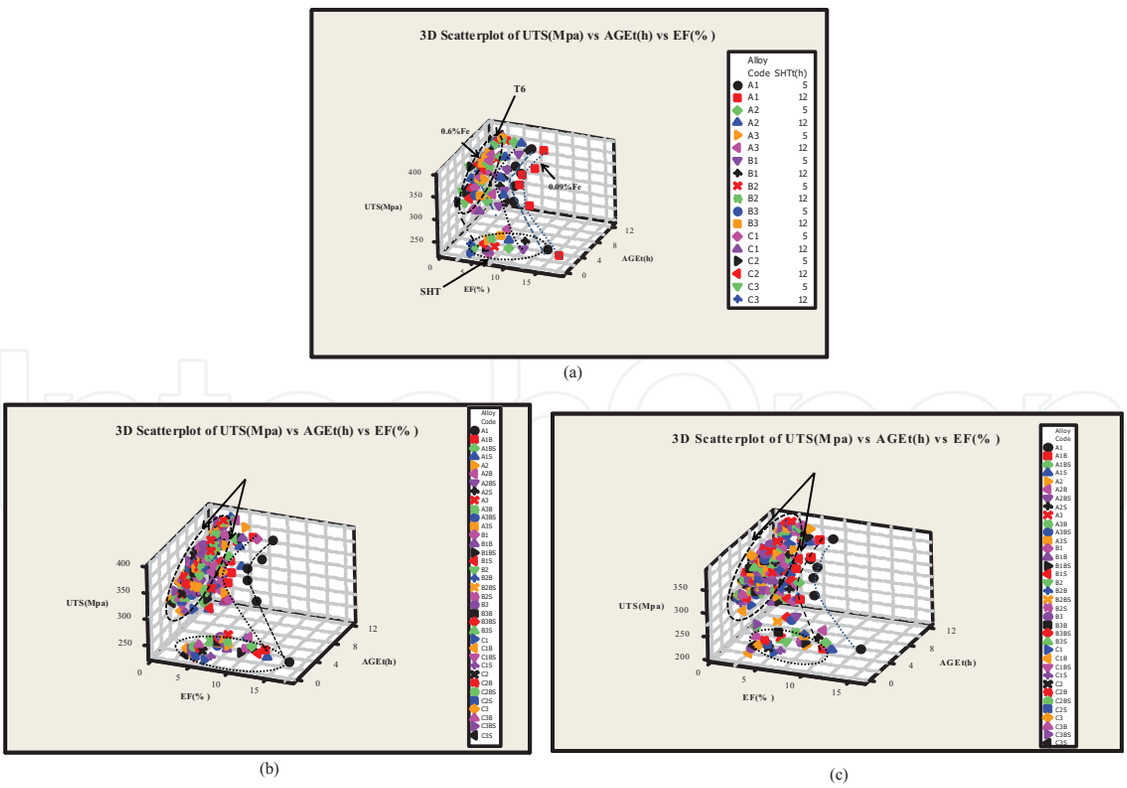

Figure 13. The 3D scattered plot of UTS versus %EF versus aging time: (a) base alloy, (b) all alloys in the T6 condition following solutionizing for 5 h at 540°C, and (c) all alloys in the T6 condition following solutionizing for 12 h at 540°C. The black arrows indicate the major axis of the oval circles.

It is evident from **Figure 13a** that Fe is the major element in determining the alloy performance. Introduction of Sr or Be or both would help in minimizing the harmful effect of Fe but to a limited extent. Increasing the solutionizing time to 12 h improved the alloy ductility due to coarsening of the eutectic Si particles. **Figure 13b** shows the UTS values of all the 36 alloys used in the present study for a solutionizing time of 5 h. It is clear that most of the T6 values are falling within a narrow zone represented by the oval circle moving the major axis to somewhat higher UTS levels with an increase in the UTS range (arrows). With increase in the solutionizing time from 5 to 12 h (**Figure 13c**), the width of the oval circle increased, accompanied by a slight drop in the major axis direction to lower UTS levels.

4. Concluding remarks

The present work was carried out on a series of heat-treatable aluminum-based aeronautical alloys containing various amounts of magnesium (Mg), iron (Fe), strontium (Sr), and beryllium (Be). From an analysis of the results obtained, the following concluding remarks may be made.

1. The addition of beryllium produces partial modification of the eutectic silicon particles in a manner similar to that reported for the addition of magnesium. The eutectic temperature was reduced by 10°C as a result of the addition of 0.8 wt% Mg. The solidification curves and their derivatives of Sr-free alloys with high Fe and Mg contents showed that there was a peak at 611°C consequent to the formation of a Be-Fe (Al_8Fe_2BeSi) phase, this peak was very close to the peak corresponding to the formation of α-Al. The morphology of the Be-Fe phase was recognized to be a script-like one.

2. Increasing the duration of solution heat treatment enhances the tensile properties of the alloys through the decomposition of the π-iron phase into the β-iron phase, fragmentation of the β-phase, and change in the geometry of both π-phase and silicon particles (i.e., spheroidization). Two mechanisms of eutectic Si particle coarsening during solution heat treatment were observed to occur: (1) Ostwald ripening in the solution and (2) clustering/collisions of the Si particles. Coarsening increases with increased solution heat treatment time.

3. Higher Mg contents are believed to be beneficial to the tensile properties (i.e., ductility, ultimate tensile strength, and yield strength) in that they oppose the detrimental effect of increasing the Fe content on the same tensile properties. Additions of Be and Sr noticeably improve the mechanical properties of the alloys with the same Fe and/or Mg contents; however, these enhancements in mechanical properties are markedly observed at higher Mg contents and reduced levels of Fe. In the case of high levels of Fe, addition of Be is preferable because it neutralizes the deleterious effects of Fe phases in cast aluminum-silicon alloys; though adding 500 ppm of Be, in case of high Fe contents, is inadequate to interact with other alloying elements. During the melting process, the possible existence of a Be-Sr phase (probably $SrBe_3O_4$) is believed to consume some of the Be content in the alloy, leading to both reduction in the free Be content as well as the alloy mechanical properties.

4. The alloy tensile properties are highly affected by varying the solutionizing and aging treatments times. In the 356 base alloy, the main strengthening effects were confirmed to be related to the formation of Mg_2Si precipitates. The improvements in the yield strength values are attributed to higher Mg contents, lower levels of Fe, addition of Be, Sr-modification, and solutionizing and aging times. Such enhancements in yield strength values are of great importance to the aeronautical industry because the design considerations in that field are mainly influenced by the yield strength.

Acknowledgements

The authors would like to thank Amal Samuel for enhancing the quality of the images and figures used in the present manuscript. They also wish to thank Dr. A.M. Samuel for careful proofreading of the manuscript.

Author details

Mohamed F. Ibrahim[1], Mohamed H. Abdelaziz[1], Herbert W. Doty[2], Salvador Valtierra[3] and Fawzy H. Samuel[1]*

*Address all correspondence to: fhsamuel@uqac.ca

1 Département des Sciences Appliquées, Université du Québec à Chicoutimi, Québec, Canada

2 General Motors, Materials Engineering, Pontiac, MI, USA

3 Nemak, S.A., Garza Garcia, N.L., Mexico

References

[1] Shivkumar S, Keller C, Trazzera M, Apelian D. Precipitation hardening in 356 alloys. In: Proceedings International Symposium on Production, Refining, Fabrication and Recycling of Light Metals; 26-30 August 1990; Hamilton, Ontario. 1990. pp. 264-278

[2] Apelian D, Shivkumar S, Sigworth G. Fundamental aspects of heat treatment of cast Al-Si-Mg alloys. AFS Transactions. 1989;**97**:727-742

[3] Edwards GA, Stiller K, Dunlop GL, Couper MJ. The precipitation sequence in Al-Mg-Si alloys. Acta Materialia. 1998;**46**(11):3893-3904

[4] Jorstad JL. Hypereutectic Al-Si casting alloys: 25 years, what's next? Silver Anniversary Paper. AFS Transactions. 1996;**104**:669-671

[5] Shivkumar S, Ricci S Jr, Steenhoff B, Apelian D, Sigworth G. An Experimental study to optimize the heat treatment of A356 alloy. AFS Transactions. 1989;**97**:791-810

[6] Yoshida KA, Arrowood RM. James. W. Evans, Microstructure and mechanical properties of A356 aluminum castings as related to various T6-Type heat treatments. In: Light Weight Alloys for Aerospace Applications III. Warrendale, PA: The Minerals, Metals, and Materials Society; 1995. p. 77-87

[7] Moustafa MA, Samuel FH, Doty HW. Effect of solution heat treatment and additives on the hardness, tensile properties and fracture behaviour of Al-Si (A413.1) automotive alloys. Journal of Materials Science. 2003;**38**:4523-4534

[8] Moustafa MA, Samuel FH, Doty HW, Valtierra S. Effect of Mg and Cu additions on the microstructural characteristics and tensile properties of Sr-modified Al-Si eutectic alloys. International Journal of Cast Metals Research. 2003;**15**:609-626

[9] Gilbert J, Leroy E. Aluminum Alloy Castings: Properties, Processes and Applications. ASM International, Materials Park, OH; 2004

[10] Barresi J, Kerr MJ, Wang H, Couper MJ. Effect of magnesium, iron and cooling rate on mechanical properties of Al-7Si-Mg foundry alloys. AFS Transactions. 2000;**114**:563-570

[11] Musmar S, Mucciardi F, Gruzleski J, Novwel A. In-situ thermal analysis technique for aluminum alloys 356, 319, Al-X Si, Al-Si-Cu X Mg, and 6063-experimental study. AFS Transaction. 2007;**115**:1-15

[12] Robison ST, Gonczy ST, Foley RD, Hartman K. Effect of different chill materials on aluminum casting solidification and mechanical properties. AFS Transactions. 2013;**121**:1-7

[13] Hatch JE. Aluminum: Properties and Physical Metallurgy. Metals Park, OH: American Society for Metals; 1984. p. 50-51

[14] Bäckerud SL, Chai G, Tamminen J. Solidification Characteristics of Aluminum Alloys. Vol. 2: Foundry Alloys. Oslo, Norway, AFS/Skanaluminium; 1990

[15] Taylor P. Ostwald ripening in emulsions. Advances in Colloid and Interface Science. 1998;**75**:107-163

[16] Samuel AM, Samuel FH, Doty HW. Observations on the formation of β-AlFeSi phase in 319 type Al-Si alloys. Journal of Materials Science. 1996;**31**:5529-5539

[17] Ibrahim MF, Samuel AM, Samuel FH, Ammar HR, Soliman M. On the impact toughness of Al-B4C MMC: the role of minor additives and heat treatment. In: 119th Metalcasting Congress, AFS 2015; 21-23 April 2015; Columbus, OH. 2015

[18] Ibrahim MF, Elgallad EM, Valtierra S, Doty HW, Samuel FH. Metallurgical parameters controlling the eutectic silicon charateristics in Be-treated Al-Si-Mg alloys. Materials. 2016;**9**(2):1-17

[19] Samuel AM, Doty HW, Valtierra S, Samuel FH. The effect of Bi-Sr and Ca-Sr interactions on the microstructure and tensile properties of Al-Si-based alloys. Materials. 2016;**9**(3):1-13

[20] Tavitas-Medrano FJ, Doty HW, Valtierra S, Samuel FH. On the enhancement of the impact toughness of A319 alloys: Role of Mg content and melt treatment. International Journal of Metalcasting. 2017;**11**(3):536-551

[21] Garza-Elizondo GH, Samuel AM, Valtierra S, Samuel FH. Effect of transition metals on the tensile properties of 354 alloy: Role of precipitation hardening. International Journal of Metalcasting. 2017;**11**(3):413-427

[22] Elsharkawi EA, Samuel FH, Simielli E, Sigworth GK. Influence of solutionizing time, modification, and cooling rate on the decomposition of Mg-containing iron intermetallic phase in 357 alloys. Transactions of the American Foundry Society. 2012;**120**:55-65 Paper No. 12-009

[23] Elsharkawi EA, Samuel E, Samuel AM, Samuel FH. Effects of Mg, Fe, Be additions and solution heat treatment on the pi-AlMgFeSi iron intermetallic phase in Al-7Si-Mg alloys. Journal of Materials Science. 2010;**45**(6):1528-1539

[24] Bailey WA, Bossing EN. High strength aluminum alloy airframe castings. AFS Transactions. 1961;**69**:660

[25] Fuoco R, Moreira M. Fatigue cracks in aluminum cylinder heads for diesel engines. International Journal of Metalcasting. 2010;**4**(4):19-32

[26] Maube SE, Wangombe DN, Maranga SM, Kihiu JM. Effect of cooling rate and heat treatment on the microstructure and impact resistance of recycled aluminum sand cast alloy. Proceeding of the Mechanical Engineering Conference. May 2012;**4**:214-218

[27] Juang SH, Wu SM. Study on mechanical properties of A356 alloys enhanced with preformed thixotropic structure. Journal of Marine Science and Technology. 2008;**16**(4): 271-274

[28] Tuttle MM, McLellan DL. Silicon particle characteristics in Al-Si-Mg castings. AFS Transactions. 1982;**90**:13-32

[29] Lados DA, Apelian D. Solution heat treatment effects on microstructure and mechanical properties of Al-(1 to 13Pct)Si-Mg cast alloys. Metallurgical and Materials Transactions B. 2011;**42B**:171-180

[30] Bailey WA. Beryllium effect on strength and mechanical properties of 356 variant—T6 aluminum alloys. AFS Transactions. 1964;**72**:443-454